David Ackland ORCID iD: 0000-0002-0559-7569

MUSCLE AND JOINT FUNCTION AFTER ANATOMIC AND REVERSE TOTAL SHOULDER ARTHROPLASTY USING A MODULAR SHOULDER PROSTHESIS

[1]David C. Ackland, [1]Wen Wu, [1]Richard Thomas, [2]Minoo Patel, [3,4]Richard Page,

[5]Morgan Sangeux, [2]Martin Richardson

[1]Department of Biomedical Engineering, University of Melbourne, Parkville, AUSTRALIA

[2]Department of Orthopaedic Surgery, Epworth Healthcare, Richmond, AUSTRALIA

[3]Department of Orthopaedic Surgery, Barwon Health, Geelong, AUSTRALIA

[4]Barwon Centre for Orthopaedic Research and Education, School of Medicine, Deakin University, Geelong, AUSTRALIA

[5]Murdoch Children's Research Institute, Parkville, AUSTRALIA

Submitted as an **Original Article** to the *Journal of Orthopaedic Research*

28th March, 2019

Address for correspondence:

David C. Ackland

Department of Biomedical Engineering

University of Melbourne

Parkville, Victoria 3010, AUSTRALIA

Phone: +613 8344 8646

Email: dackland@unimelb.edu.au

Running title: Muscle and joint function after shoulder arthroplasty

Author contribution statement: DA assisted with experiments, performed data analysis and drafted manuscript; WW performed musculoskeletal modeling; RT performed experiments; MP performed arthroplasties; RP assisted with manuscript writing; MS assisted with modeling analysis; MR performed arthroplasties. All authors have read and approved the final submitted manuscript.

ABSTRACT

Changes in joint architecture and muscle loading resulting from total shoulder arthroplasty (TSA) and reverse total shoulder arthroplasty (RSA) are known to influence joint stability and prosthesis survivorship. This study aimed to measure changes in muscle moment arms, muscle lines of action, as well as muscle and joint loading following TSA and RSA using a metal-backed uncemented modular shoulder prosthesis. Eight cadaveric upper extremities were assessed using a customized testing rig. Abduction, flexion and axial rotation muscle moment arms were quantified using the tendon-excursion method, and muscle line-of-force directions evaluated radiographically pre-operatively, and after TSA and revision RSA. Specimen-specific musculoskeletal models were used to estimate muscle and joint loading pre- and post-operatively. TSA lateralized the glenohumeral joint center by 4.3 ± 3.2 mm, resulting in small but significant increases in middle deltoid force (2.0%BW) and joint compression during flexion (2.1%BW) ($p<0.05$). Revision RSA significantly increased the moment arms of the major abductors, flexors, adductors and extensors, and reduced their peak forces ($p<0.05$). The superior inclination of the deltoid significantly increased while the inferior inclination of the rotator cuff muscles decreased ($p<0.05$). TSA using an uncemented metal-backed modular shoulder prosthesis effectively restores native joint function; however, lateralization of the glenoid component should be minimised intra-operatively to mitigate

increased glenohumeral joint loading and polyethylene liner contact stresses. Revision RSA reduces muscle forces required during shoulder function but produces greater superior joint shear and less joint compression. The findings may help to guide component selection and placement to mitigate joint instability after arthroplasty.

Keywords: rotator cuff; deltoid; glenohumeral; joint torque; joint force; upper limb; musculoskeletal model

INTRODUCTION

Total shoulder arthroplasty (TSA) is an established treatment for cases of advanced glenohumeral joint osteoarthritis, with pain relief, functional improvements and high survivorship reported in patients with an intact rotator cuff[1-3]; however, revision surgery rates due to failure of glenoid component fixation have continued to increase[4], and long-term stability of the glenoid component remains a challenge. TSA using non-cemented metal-backed glenoid components provides greater initial fixation strength than that of cemented all-polyethylene glenoid components but has been associated with three-time greater revision rates in early metal back implants[5,6]. It is thought that lateralization of the glenoid component may increase the load generated by the musculature, leading to larger joint forces with the potential for accelerated polyethylene wear[7]. At present, there is little biomechanical data available on the joint lateralisation that occurs after TSA using modern metal-backed glenoid components, and how this influences muscle and joint force production.

Reverse total shoulder arthroplasty (RSA) represents three quarters of all shoulder arthroplasty procedures[8], with rotator cuff tears and arthritis present in 80% of cases[9];

however, the indications for RSA extend to 3- and 4-part proximal humeral fractures[10], pseudoparesis[11], rheumatoid arthritis[12], and revision arthroplasty[13]. Functionally, RSA has been shown to medialize the glenohumeral joint center, increase the leverage and tension in the deltoid, recruit more of its fibres during abduction and flexion, and improve range of upper limb motion and glenohumeral joint stability[14,15]. The development of modular prostheses now allows ease of conversion from conventional TSA to RSA by eliminating the need to remove well-fixed glenoid- or humeral-side components, which otherwise risks bone loss, fracture, and poor survivorship[16-18]. While clinical studies have shown the modular shoulder prosthesis to minimize morbidity and reduce rates of complication following revision to RSA[19], biomechanical changes in muscle and joint loading from TSA to revision RSA have not been quantified to date. The magnitude and direction of the forces produced by the musculature after arthroplasty are clinically significant, as they give rise to the glenohumeral joint force which, when compressive, stabilizes the joint by concavity compression, or when predominantly shear-based, may lead to joint instability and subluxation.

The aims of the present study were threefold. Firstly, to evaluate in a human cadaveric model the changes in the glenohumeral joint center and humerus position after TSA and revision RSA using a modular shoulder prosthesis; secondly, to quantify after TSA and RSA the abduction, flexion and axial rotation muscle moment arms and the orientation of the muscle lines of action in the shoulder; and third, to employ computational modelling to evaluate muscle and joint forces during these tasks pre- and post-operatively. The moment arm of a muscle represents its torque capacity and is defined by the perpendicular distance between its line of action and the joint center of rotation in a given plane of motion. Since TSA and RSA in metal-backed glenoid prosthesis designs are known to change the location of the glenohumeral joint center of rotation relative to that in the native shoulder, we hypothesised that muscle lines of action and moment arms, and therefore the muscle forces and glenohumeral joint forces, would be impacted post-operatively.

MATERIALS AND METHODS

Specimen preparation

Eight fresh-frozen human cadaveric entire upper extremities were arthroscopically screened for bone and joint degeneration (mean body weight: 69.5 kg; body weight range: 50.8 kg-102.1 kg; mean age: 68 years; age range: 56-75 years; 6 male, 2 female). This sample size has been shown to produce a study power of >0.8 in detecting significant differences in muscle moment arms and joint-contact loading before and after RSA, with α=0.05[20,21]. The upper limb was disarticulated, and the skin and subcutaneous tissues proximal to the glenohumeral joint removed by sharp dissection. The proximal origins of the major scapulohumeral muscles identified and divided into the following sub-regions: The subscapularis (inferior, middle, superior – three equal portions from the inferior, middle and superior subscapular fossa); supraspinatus (anterior, posterior – two equal halves from the supraspinous fossa); infraspinatus (superior, inferior – two equal halves from the infraspinous fossa); the deltoid (anterior – clavicular fibers; middle – acromion fibers; posterior – posterior scapula spine fibers). The teres minor was treated as one functional unit. The origins of each muscle were detached and their bony centroids of attachment marked on the scapula or clavicle with pins. All muscle were resected and loops of suture (5-Ethibond, Jonson & Jonson, USA) secured to the proximal tendons. The clavicle, elbow and wrist joints were fused in an approximate neutral position using Steinmann pins.

Experimental apparatus and testing protocol

Each upper limb specimen was mounted onto a custom-designed testing apparatus (Fig. 1). The scapula was embedded in a hollow mounting block using dental cement with the plane of the glenoid aligned with the vertical. To maintain muscle-tendon unit tension while minimising load-induced muscle-tendon lengthening, and to assist in producing joint congruency during testing, nylon lines were attached to the suture of each proximal tendon and passed through a perforated plate to a free-hanging weight of 5 N. Each tendon unit was pulled toward the centroid of its proximal origin, thus reproducing the approximate line of action of the muscle-tendon unit.

Joint motion was quantified using a 4-camera video motion analysis system (Vicon Motion System, UK) by tracking triads of retro-reflective markers on Steinmann pins inserted into the scapula and humerus. ISB-recommended scapula and humeral coordinate systems were defined relative to bony landmarks that were digitised using a custom-made hand-held passive marker wand[20,21]. The glenohumeral joint centre was calculated by moving the upper limb through its range of motion for 20 seconds and computing a humerus-fixed virtual point of minimum translation. Retro-reflective markers were also placed above each free weight so that their vertical displacements, resulting from tendon excursion, could be measured by the motion capture system. Video motion data were sampled at 100 Hz.

The humerus of each specimen was passively abducted from the neutral position (approximately 0^o abduction) to full abduction, then adducted back to the neutral position. This cycle was performed 10 times to assess repeatability, and the elevation procedure was then repeated in the sagittal plane (flexion). With the humerus in 45^o of abduction, cycles of axial rotation were also performed through full internal and external rotation. Abduction was defined in the plane of the scapula (scaption), while flexion was in the saggital-plane, which was defined 60^o anterior to the scapula plane. Muscle moment arms during abduction, flexion and axial rotation motions were calculated using the tendon excursion method. Specifically, tendon-excursion and joint angle data were averaged across three consecutive cycles, and each muscle's moment arms were computed from the gradient of the plot of tendon excursion vs joint angle. Moment arm data were normalized to humeral head radius, which was determined from scapular plane radiographs. This was achieved by multiplying each moment arm by the ratio of the average humeral head radius of all specimens to the humeral head radius of the given specimen [20,21]. Moment arm data were smoothed using a 4^{th} order, low-pass Butterworth filter with a cut-off frequency of 5 Hz. A similar filter has been adopted in other human movement research[22].

The line of action of each muscle-tendon unit was calculated in the scapular plane at 0^o, 45^o and 90^o of abduction, as well as at 45^o and 90^o of flexion. This was achieved by attaching a metal wire to the suture of each tendon and pulling the wire toward the muscle-tendon unit's proximal origin using a 10N free-hanging weight. Specimens were radiographed using x-ray fluoroscopy at each joint position (Fluoroscan InSight 2, Hologic Inc. Bedford, MA), and each muscle line of action was calculated from its wire orientation with respect to the glenoid plane of the base-plate (Fig. 2). A muscle's line of action is defined from the directional cosines of the vector formed between the most proximal tendon wrapping 'via point' (where the tendon loses contact with the humerus) and the centroid of tendon origin[23].

Muscle moment arm and line of action measurements were first performed in the native shoulder and were repeated after anatomic TSA, as then revision RSA. Shoulder arthroplasties were performed using an uncemented modular metal-backed prosthesis (SMR System, Lima Corporate, Italy) following the manufacturer's technique. Glenoid reaming removed cartilage down to subchondral bone and the metal back glenoid was fixed with a press-fit central peg and two screws. Humeral head components ranged in size from 42mm to 50mm, and their rotational offsets were trialed and matched to the native anatomy using x-ray fluoroscopy to ensure they were correctly sized and orientated. Humeral stems ranged in size between 16 mm and 23 mm. The distance between the trigonum spinae of the scapula and the glenohumeral joint centre was measured in each specimen and used to estimate changes in joint position after TSA and RSA. The position of the humerus after TSA and RSA was measured radiographically in the scapular-plane in its neutral position (Fig. 2). The mediolateral and superioinferior position of the humeral stem was expressed relative to a coordinate system centred and aligned with the glenoid plane of the base-plate. Specimens were frequently irrigated with saline during testing.

Musculoskeletal modelling

Dynamic simulations of abduction, flexion, and external rotation with the humerus in 45° abduction, were performed in the native shoulder, as well as the shoulder after TSA and RSA. Specimen-specific rigid-body musculoskeletal models of each native upper extremity were first developed based on a previously published generic upper limb computational model developed in OpenSim[24]. Briefly, the glenohumeral and acromioclavicular joints were modelled as 3-degree-of-freedom (DOF) ball and socket joints, the sternoclavicular joint as a 2-DOF universal joint, and the elbow joint as a 2-DOF universal joint. Humeral motion was actuated by 26 Hill-type muscle-tendon units. Segment lengths, mass, center of mass location and inertial properties were scaled to match each specimen using previously published data[25]. Optimization was used to calculate the optimal muscle paths in order to match the model's muscle moment arms and lines of action with those measured previously on cadaveric upper extremities[20,26]. To achieve this, muscle paths were initially determined using the anatomy of the Visible Human Male for the neutral position, and then wrapping objects and 'via point' locations were iterated until an optimal solution throughout the range of abduction and flexion was obtained.

Joint angles during simulations were based on average upper limb kinematics measured in six healthy male subjects (mass: 56–85 kg; height: 170–175 cm; age: 25–38 yrs)[24,27]. Muscle forces were computed using static optimisation by minimizing the sum of the squares of muscle activations subject to constraints on each muscle's force-length and force-velocity relations, as well as on the glenohumeral joint force direction. To simulate glenohumeral joint anatomy after TSA and RSA, the joint centre of rotation and humeral positions were prescribed based on specimen-specific measurements (Fig. 3). While this produced new muscle moment arms, lines of action and muscle-tendon unit lengths in each case, these quantities were not optimised to the specimen-specific measurements. Since supraspinatus tears present more frequently than any other rotator cuff tendon tear[28], a full-thickness supraspinatus tear was simulated by removing the entire muscle-tendon unit from the reverse shoulder models.

Data analysis

A 1-way multivariate analysis of variance (MANOVA) was used to assess the influence of TSA and RSA on peak muscle moment arms and the joint angles at which they occur. The dependent variables were maximum moment arm and joint angle, while the independent variable was shoulder state (native, anatomic and reverse shoulder). A 2-way MANOVA was used to quantify the influence of shoulder state and joint angles on muscle lines of action, as well as their interaction, and a further 1-way MANOVA used to assess the influence of shoulder state on average and maximum muscle forces and glenohumeral joint forces. Games-Howell post-hoc tests were employed for non-parametric data, and Shapiro-Wilk tests used to assess normality of data. Standard deviation was used as a measure of the dispersion of the results, and significance level was set at $p<0.05$. All statistical analysis was performed using the statistical package for Social Science (PASW Statistics 18, SPSS Inc, Chicago, IL).

RESULTS

Glenohumeral joint geometry

TSA lateralized the glenohumeral joint centre of rotation by 4.3 ± 3.2 mm relative to that in the native shoulder. RSA medialized and inferiorised the glenohumeral joint centre of rotation relative to that in the anatomical shoulder by 25.8 ± 6.3 and 16.4 ± 3.9 mm, respectively.

Muscle moment arms

There were no significant differences in the peak abduction and flexion moment arms of the shoulder muscles after anatomic TSA relative to those in the native shoulder (Table 1), nor significant differences in the peak external rotation moment arms (Table 2) ($p>0.05$).

After revising the anatomic shoulder to a reverse prosthesis, there was an increase in the peak abduction moment arms of the anterior deltoid (mean increase: 9.8 mm, 95% CI: [0.6, 19.0], $p=0.036$) and middle deltoid (mean increase: 13.3 mm, 95% CI: [3.1, 23.4], $p=0.011$), and a decrease in the peak adduction moment arm of the posterior deltoid (mean decrease: 18.1 mm, 95% CI: [5.16, 31.08], $p=0.009$) (Table 1). There was also a decrease in the peak abduction moment arm of the superior infraspinatus after RSA (mean decrease: 7.7 mm, 95% CI: [1.8, 13.6], $p=0.021$) and an increase in the peak adduction moment arm of the inferior subscapularis (mean increase: 15.2 mm, 95% CI: [3.3, 27.1], $p=0.012$) and teres minor (mean difference: 12.2 mm, 95% CI: [2.7, 21.7], $p=0.021$).

Compared to those in the anatomic shoulder, the peak flexion moment arms after RSA were significantly larger in the middle deltoid (mean difference: 21.5 mm, 95% CI [0.3, 42.8], $p=0.047$), while the peak extension moment arm of the posterior deltoid was significantly lower (mean difference: 11.3 mm, 95% CI [0.1, 22.5], $p=0.009$). There were no significant differences in the joint angles at which the peak moment arms occurred during abduction and flexion ($p>0.05$). After RSA, the peak internal rotation moment arms were found to be significantly smaller in the superior subscapularis sub-region during axial rotation at 45^o of abduction (mean difference: 4.11 mm, 95% CI [0.23, 7.98], $p=0.037$) and the middle subscapularis during axial rotation at 45^o of flexion (mean difference: 9.08 mm, 95% CI [0.82, 17.34], $p=0.033$).

Muscle lines of action

There were no significant changes in the scapular-plane muscle lines of action after TSA ($p>0.05$) (Table 3). After RSA, the lines of action of the deltoid sub-regions were more superiorly inclined relative to those in the anatomic shoulder, while the rotator cuff muscle sub-regions were less inferiorly inclined (Fig. 4). There were significant increases in the middle deltoid line of action inclination at 0^o of abduction (mean difference: 14.7^o, 95% CI [2.1, 27.3], $p=0.025$), 45^o of abduction (mean difference: 13.8^o, 95% CI [1.6, 26.0], $p=0.030$), 90^o of abduction (mean difference: 16.7^o, 95% CI [4.2, 29.2], $p=0.013$), and 45^o of flexion after RSA (mean difference: 19.73^o, 95% CI [5.9, 33.5], $p=0.008$). The superior subscapularis line of action after RSA was significantly less inferiorly inclined at 0^o, 45^o and 90^o of abduction (mean difference: 17.69^o, 11.51^o, 17.53^o, respectively) as well as at 45^o and 90^o of flexion (mean difference: 16.4^o and 20.6^o, respectively) ($p<0.05$). The line of action of the superior infraspinatus was significantly less inferiorly inclined at 0^{o} and 45^{o} of abduction (mean difference: 12.09^{o} and 11.49^{o}, respectively) ($p<0.05$)

Muscle forces

With the exception of the posterior deltoid, there were small but significant changes in peak and average forces of all shoulder muscles after TSA, relative to those in the native shoulder ($p<0.05$). After TSA during flexion, the middle deltoid demonstrated a larger average force (mean difference: 2.0%BW, 95%CI: [0.5, 3.6], p=0.001) (Table 4) and peak force (mean difference: 3.1%BW, 95% confidence interval: [0.7, 5.5], p=0.008) (Table 5). A decrease in the peak subscapularis force (mean difference: 5.0%BW, 95%CI: [1.6 8.4], $p<0.001$) and infraspinatus force (mean difference: 4.5%BW, 95%CI: [1.4, 7.6], $p<0.001$) was observed during abduction (Fig. 5). After TSA, the average (maximum) forces in the teres minor, trapezius, pectoralis major, seratus anterior and rhomboids minor were significantly larger by up to 0.7%BW (1.3%BW) during abduction, flexion (Fig. 6) and rotation ($p<0.05$) (Fig. 7).

After revising the anatomic shoulder to a reverse prosthesis, there was a significantly smaller peak force during abduction, flexion and rotation generated by the middle deltoid (mean difference: 16.1%BW, 11.4%BW, 3.1%BW, respectively), subscapularis (mean difference: 32.5%BW, 17.1%BW and 23.8%BW, respectively) and infraspinatus (mean increase: 21.3%BW, 13.5%BW and 6.1%BW, respectively) ($p<0.001$). In contrast, the average pectoralis major force was significantly larger during abduction, flexion and rotation (mean difference: 9.8%BW, 6.5%BW and 10.2%BW, respectively) ($p<0.001$).

Glenohumeral joint forces

After TSA, there was a significantly larger average glenohumeral joint force (mean difference: 2.6%BW, 95%CI: [0.5, 4.7], $p=0.020$) and peak glenohumeral joint force magnitude during flexion (mean difference: 4.0%BW, 95%CI: [0.7, 7.2], $p<0.009$) relative to that in the native shoulder (Fig. 6). This was associated with a significantly greater average compressive component of the glenohumeral joint force (mean difference: 2.1%BW, [0.4, 3.8], $p=0.021$) and an increase in the average superior component of the glenohumeral joint force during flexion (mean difference: 2.8%BW, [0.7, 4.9], $p=0.013$) (Table 4). Similarly, a larger average glenohumeral joint force magnitude, greater compressive component of the glenohumeral joint force, and smaller superior component of the glenohumeral joint force was observed during external rotation ($p<0.05$) (Fig. 7).

After revision RSA, the magnitude of the average glenohumeral joint force was significantly smaller during abduction (mean difference: 32.3%BW, 95%CI: [27.1, 38.7], $p<0.001$), flexion (mean difference: 15.8%BW, 95%CI: [8.5, 23.1], $p=0.001$) and rotation (mean difference: 11.7%BW, 95%CI: [5.2, 18.2], $p = 0.002$). This was associated with a significantly smaller average compressive component of the glenohumeral joint force (45.4%BW, 28.2%BW and 22.8%BW during abduction, flexion and rotation, respectively) ($p<0.001$), and a significant increase in the average superior component of the glenohumeral joint force (4.7%BW, 7.2%BW and 9.1%BW during abduction, flexion and rotation, respectively) ($p<0.001$).

DISCUSSION

TSA using uncemented metal-backed glenoid components is known to provide high fixation strength and reduce glenoid lucent lines, which have been observed in up to 90% of cemented all-polyethylene implants. A study reporting a 46% revision-free survival rate of an early design metal-backed total shoulder replacement at 12 years suggested evidence of soft tissue deficiency, accelerated polyethylene wear, and glenoid loosening associated with osteolysis secondary to wear debris[5]. New generation cementless metal-backed implants with modular components facilitate ease of revision from primary anatomical to reverse shoulder and have demonstrated 100% survivorship at 6.3 years, with no evidence of loosening reported at the humeral stem and glenoid baseplate[29]. Concerns about post-operative rotator cuff tearing and higher revision rates in metal-backed glenoid components compared to those in cemented glenoids has underpinned a need for quantitative muscle and joint function data following TSA[30].

Changes in glenohumeral joint centre of rotation position directly affect a spanning muscle's moment arm in a given plane of motion, and therefore the leverage and torque-producing potential of the muscle. After revision RSA, an average 25.8 mm medialization of the glenohumeral joint centre contributed to significant increases in the maximum abduction moment arms of the anterior deltoid, middle deltoid, posterior deltoid, and the adduction moment arms of the inferior subscapularis, superior infraspinatus and teres minor, as well as decreases in peak forces generated by these muscles. Lower muscle forces for a given elevation increase the efficiency of muscle-actuated joint movements and may ultimately contribute to improved range of motion observed clinically[29]; however, when humerus position changes following RSA, muscles spanning the glenohumeral joint and inserting on the humerus may lengthen or shorten, shifting the operating region on their force-length curve and altering their force-producing potential.

Anatomic TSA lateralised the joint centre of rotation by an average 4.3 mm, which was a consequence of the combined geometry at both the glenoid and humeral sides and influenced by the thickness of the metal back and liner construct, depth of the glenoid reaming, and matching of the prosthetic humeral head to the native bone. The results indicate that the anatomic prosthesis replicated the native joint anatomy without substantially altering muscle moment arms and lines of action; however, there were small but significant changes in the forces produced by a number of muscles, as well as an increase in the average and peak magnitude of the glenohumeral joint force during flexion (2.6%BW and 4%BW for the average and peak glenohumeral joint force, respectively). The middle deltoid produced an average 2%BW more force during flexion after TSA compared to that in the native shoulder, which was more than that of any other shoulder muscle. The increase in middle deltoid muscle-tendon unit length is likely to have shifted the operating region of this muscle further up the ascending region of the force-length curve, resulting in an increase in its force production. Consequently, lengthening of the middle deltoid following TSA contributed primarily to the observed increases in joint force. Larger glenoid offset from the metal backing may incur increased stresses on the polyethylene liner, ultimately contributing to component wear. In addition, increased rotator cuff muscle-tendon loading may present greater risk of post-operative rotator cuff tearing[30]. While the present study does not conclude decreased survivorship in metal-backed glenoids following TSA, the findings suggest that minimizing joint lateralization may help to preserve the native muscle force-length operating characteristics and joint loading.

Dislocation is the most common cause of revision TSA[7], and has been shown to account for up to 44% of all complications associated with RSA; however, its etiology, which is thought to involve prior surgery, bone deficiency, rotator cuff tears, trauma and mechanical factors, is poorly understood[31]. Change in humeral position following RSA, relative to the anatomic shoulder, was shown to substantially affect lines of action of shoulder muscles and thus their joint compressive and shear potential, which ultimately influences joint stability. The results suggest the average superior component of the glenohumeral joint force in the reverse shoulder was significantly larger than that in the native and anatomic shoulder during abduction, flexion and axial rotation, despite substantial decreases in the average forces produced by the rotator cuff and middle deltoid following RSA.

The deltoid became more superiorly inclined after RSA, with maximum obliquity in the neutral position and the middle deltoid line of action just 15° off vertical orientation (Fig. 4). Because the middle and anterior deltoid are the major force producers and most superiorly inclined after RSA, they contribute most of the superior glenohumeral joint shear. The reduced rotator cuff depressor function observed following RSA provides less resistance to the shear forces generated by the deltoid, leading to greater overall superior glenohumeral joint shear. This large joint shear force, particularly when the arm is at rest by the side, may be a factor in early revision surgery following RSA. While large muscle-generated joint shear forces during activities of daily living appear to be prevalent after RSA, they are resisted by the semi-constrained anatomy of the articular surfaces and predominantly transmitted to the base-plate. However, loss of antagonist muscle function with large rotator cuff tears may exacerbate superior joint shear production, resulting in increased risk of joint subluxation, particularly in the case of an over- or under-tensioned deltoid.

We showed a maximum middle deltoid abduction moment arm of 42.1 mm after RSA, which compares to cadaveric measurements using the Zimmer-Biomet trabecular metal reverse shoulder system (46.2 mm)[21], and model calculations by Terrier et al (2008) using the Tornier reversed Aequalis (48.0 mm)[32]. However, Terrier et al employed a single subject in the computational model development, and the elderly cadaveric specimens used in the present study may have had reduced muscle mass leading to smaller moment arm quantities. Experimentally derived tendon-excursion data is also sensitive to changes in muscle lines of action, bone geometry, joint centre of rotation location and measurement technique, all of which has contributed to large variance in previously reported measured shoulder muscle moment arm quantities[33].

The present study demonstrated that after RSA at 0° of abduction, the anterior deltoid was inclined at an angle of 156° while the middle deltoid was inclined at an angle of 166°. Measurements made by digitizing muscle paths on cadaveric specimens yielded 150° and 165° for the anterior and middle deltoid, respectively[34]. However, we believe our technique of radiographically quantifying the line of action of muscle-tendon units using radio-opaque wires may improve on measurement strategies that depend on superficial visualization of wrapping ‘via points’ from the gross shoulder anatomy, since muscle paths and bone-wrapping may be more readily identified in an anatomical plane. Our estimate of average middle deltoid force during flexion of the native shoulder (93 N) was similar to that calculated by Masjedi and Johnson (2010)[35] during reaching (87 N). However, our sum of forces of each deltoid sub-region at 60° abduction was 37.0%BW (252 N), which was larger than that measured experimentally in a cadaveric model[36] (201 N), possibly due to the different prosthesis, alignment and muscle architecture. We also reported a peak glenohumeral joint force during abduction in the reverse shoulder of 43%BW, and this was of similar magnitude to that calculated by Kontaxis and Johnson (2009) using a musculoskeletal model (49%BW)[37], and by Ackland et al. (2018) using a finite element model (53% BW)[38].

There are limitations of this study. First, there may have been joint translation during tendon excursion experiments, and this could have generated false tendon excursion resulting in moment arm errors; however, joint translation was minimized with constant muscle-tendon unit loading, and by the semi-constrained reverse shoulder articulation. Conversely, the musculoskeletal model simulations assumed the glenohumeral joint to be a constrained 3-DOF ball-and-socket; however, active shoulder abduction and flexion has been shown to result in <2mm of humeral translation[39], and such joint motion is unlikely to have substantial influence on muscle and joint force calculations. Second, the present study considered an intact rotator cuff for the native and anatomic shoulder, and an isolated full-thickness supraspinatus tear in the reverse shoulder. Rotator cuff tears involving other tendons are likely to influence muscle recruitment, joint loading and adversely affect joint stability[38]. Musculotendon parameters were also derived from a healthy male subject and may overestimate the strength and function of muscles in an osteoarthritic patient. Third, transverse plane muscle lines of action were not measured post-operatively, but ought to be the focus of future research. Finally, muscle and joint loading calculations were not directly validated; however, each specimen-specific musculoskeletal model was based on a previously published native shoulder model with muscle moment arms and lines of action previously measured and validated on upper limbs of similar age, muscle force-length and force-velocity profiles quantified using strength-data from healthy adults, timing of muscle activation validated against measured electromyography (EMG), and joint force calculations validated against instrumented implant data[24,27,40].

The results of the present study suggest that the observed statistical differences in outcome variables between the native, anatomic and reverse shoulders were associated with substantial biomechanical changes. For instance, the peak glenohumeral joint force after revision TSA increased significantly by 4.0%BW (approximately 27.2 N) during flexion, while the standard deviation of joint force in the native shoulder was 0.3%BW. For the primary muscle and joint force measures, the significant between-group difference reported were in general one order of magnitude larger than the between-subject variance, suggesting a biomechanically relevant change in joint function. Furthermore, the significant differences in measured peak elevation muscle moment arms between the anatomic and reverse shoulder varied from 7.7 mm (superior infraspinatus during abduction) to 21.5 mm (middle deltoid during flexion). The combined changes in moment arms of these and other shoulder muscles are likely to be the primary contributor to the marked differences in estimated muscle recruitment patterns and glenohumeral joint force following RSA, which have been shown to be clinically relevant[41].

In conclusion, TSA using a cementless metal-backed modular shoulder prosthesis effectively restores native joint function; however, this procedure may lateralise the glenohumeral joint centre of rotation, increasing middle deltoid muscle force generation and resulting in larger glenohumeral joint compressive forces during flexion. These findings may be generalized to other modular or non-modular shoulder prostheses that lateralise the glenohumeral joint. Minimizing joint lateralization intra-operatively may help to mitigate joint-contact stresses that are believed to contribute to accelerated polyethylene liner wear; however, further research is required to link joint force with component wear rates. Revision RSA medializes the glenohumeral joint centre, and medializes and inferiorises the humerus with respect to that in the anatomical shoulder, a finding that is also likely to be applicable to non-modular reverse shoulder prosthesis designs. This increases the moment arms of the major abductors, flexors, adductors and extensors, resulting in reduced peak forces produced by these muscles, and more efficient muscle and joint function. The superior inclination of the deltoid increases and the inferior inclination of the rotator cuff muscles decrease, contributing to greater superior glenohumeral joint shear and less joint compression following RSA. The findings may help to guide component selection and placement to mitigate joint instability after shoulder arthroplasty.

ACKNOWLEDGEMENTS

This project was partially funded by Lima Corporate, Italy, who exercised no control over the study design or data analysis.

REFERENCES

1. Deshmukh AV, Koris M, Zurakowski D, et al. 2005. Total shoulder arthroplasty: long-term survivorship, functional outcome, and quality of life. J Shoulder Elbow Surg 14:471-479.

2. Montoya F, Magosch P, Scheiderer B, et al. 2013. Midterm results of a total shoulder prosthesis fixed with a cementless glenoid component. J Shoulder Elbow Surg 22:628-635.

3. Torchia ME, Cofield RH, Settergren CR. 1997. Total shoulder arthroplasty with the Neer prosthesis: long-term results. J Shoulder Elbow Surg 6:495-505.

4. Day JS, Lau E, Ong KL, et al. 2010. Prevalence and projections of total shoulder and elbow arthroplasty in the United States to 2015. J Shoulder Elbow Surg 19:1115-1120.

5. Boileau P, Moineau G, Morin-Salvo N, et al. 2015. Metal-backed glenoid implant with polyethylene insert is not a viable long-term therapeutic option. J Shoulder Elbow Surg 24:1534-1543.

6. Gauci MO, Bonnevialle N, Moineau G, et al. 2018. Anatomical total shoulder arthroplasty in young patients with osteoarthritis. Bone Joint J 100-B:485-492.

7. Page R, Pai V, Eng K, et al. 2018. Cementless versus cemented 1 glenoid components in conventional total shoulder joint arthroplasty: Analysis from the Australian Orthopaedic Association National Joint Replacement Registry (AOANJRR). J Shoulder Elbow Surg In Press.

8. 2018. Australian Orthopaedic Association National Joint Replacement Registry (AOANJRR). Annual Report (2018).

9. Schairer WW, Nwachukwu BU, Lyman S, et al. 2015. National utilization of reverse total shoulder arthroplasty in the United States. J Shoulder Elbow Surg 24:91-97.

10. Bufquin T, Hersan A, Hubert L, et al. 2007. Reverse shoulder arthroplasty for the treatment of three- and four-part fractures of the proximal humerus in the elderly: a prospective review of 43 cases with a short-term follow-up. J Bone Joint Surg Br 89:516-520.

11. Werner CM, Steinmann PA, Gilbart M, et al. 2005. Treatment of painful pseudoparesis due to irreparable rotator cuff dysfunction with the Delta III reverse-ball-and-socket total shoulder prosthesis. J Bone Joint Surg Am 87:1476-1486.

12. John M, Pap G, Angst F, et al. 2010. Short-term results after reversed shoulder arthroplasty (Delta III) in patients with rheumatoid arthritis and irreparable rotator cuff tear. Int Orthop 34:71-77.

13. Levy JC, Virani N, Pupello D, et al. 2007. Use of the reverse shoulder prosthesis for the treatment of failed hemiarthroplasty in patients with glenohumeral arthritis and rotator cuff deficiency. J Bone Joint Surg Br 89:189-195.

14. Boileau P, Watkinson DJ, Hatzidakis AM, et al. 2005. Grammont reverse prosthesis: design, rationale, and biomechanics. J Shoulder Elbow Surg 14:147S-161S.

15. Ackland DC, Patel M, Knox D. 2015. Prosthesis design and placement in reverse total shoulder arthroplasty. J Orthop Surg Res 10:101.

16. Flury MP, Frey P, Goldhahn J, et al. 2011. Reverse shoulder arthroplasty as a salvage procedure for failed conventional shoulder replacement due to cuff failure--midterm results. Int Orthop 35:53-60.

17. Ortmaier R, Resch H, Matis N, et al. 2013. Reverse shoulder arthroplasty in revision of failed shoulder arthroplasty-outcome and follow-up. Int Orthop 37:67-75.

18. Van Thiel GS, Halloran JP, Twigg S, et al. 2011. The vertical humeral osteotomy for stem removal in revision shoulder arthroplasty: results and technique. J Shoulder Elbow Surg 20:1248-1254.

19. Weber-Spickschen TS, Alfke D, Agneskirchner JD. 2015. The use of a modular system to convert an anatomical total shoulder arthroplasty to a reverse shoulder arthroplasty: Clinical and radiological results. Bone Joint J 97-B:1662-1667.

20. Ackland DC, Pak P, Richardson M, et al. 2008. Moment arms of the muscles crossing the anatomical shoulder. J Anat 213:383-390.

21. Ackland DC, Roshan-Zamir S, Richardson M, et al. 2010. Moment arms of the shoulder musculature after reverse total shoulder arthroplasty. J Bone Joint Surg Am 92:1221-1230.

22. Li K, Ackland DC, McClelland JA, et al. 2012. Trunk muscle action compensates for reduced quadriceps force during walking after total knee arthroplasty. Gait Posture 38(1):79-85.

23. Ackland DC, Pandy MG. 2009. Lines of action and stabilizing potential of the shoulder musculature. J Anat 215:184-197.

24. Wu W, Lee PV, Bryant A, et al. 2016. Subject-specific musculoskeletal modeling in the evaluation of shoulder muscle and joint function. J Biomech 49:3623-3634.

25. S. P, Evans FG, T. A. 1983. Anatomical Data for Analyzing Human Motion. Research Quarterly Exercise Sport 54:169-178.

26. Ackland DC, Pandy MG. 2011. Moment arms of the shoulder muscles during axial rotation. J Orthop Res 29:658-667.

27. Wu W, Lee PV, Ackland DC. 2017. The sensitivity of shoulder muscle and joint force predictions to changes in joint kinematics: A Monte-Carlo analysis. Gait Posture 54:87-92.

28. Hattrup SJ, Cofield RH, Cha SS. 2006. Rotator cuff repair after shoulder replacement. J Shoulder Elbow Surg 15:78-83.

29. Castagna A, Delcogliano M, de Caro F, et al. 2013. Conversion of shoulder arthroplasty to reverse implants: clinical and radiological results using a modular system. Int Orthop 37:1297-1305.

30. Thomas R, Richardson M, Patel M, et al. 2018. Rotator cuff contact pressures at the tendon-implant interface after anatomic total shoulder arthroplasty using a metal-backed glenoid component. J Shoulder Elbow Surg 27:2085-2092.

31. Edwards TB, Williams MD, Labriola JE, et al. 2009. Subscapularis insufficiency and the risk of shoulder dislocation after reverse shoulder arthroplasty. J Shoulder Elbow Surg 18:892-896.

32. Terrier A, Reist A, Merlini F, et al. 2008. Simulated joint and muscle forces in reversed and anatomic shoulder prostheses. J Bone Joint Surg Br 90:751-756.

33. Hik F, Ackland DC. 2019. The moment arms of the muscles spanning the glenohumeral joint: a systematic review. J Anat 234:1-15.

34. Ackland DC, Roshan-Zamir S, Richardson M, et al. 2011. Muscle and joint-contact loading at the glenohumeral joint after reverse total shoulder arthroplasty. J Orthop Res 29:1850-1858.

35. Masjedi M, Johnson GR. 2010. Glenohumeral contact forces in reversed anatomy shoulder replacement. J Biomech 43:2493-2500.

36. Henninger HB, Barg A, Anderson AE, et al. 2012. Effect of deltoid tension and humeral version in reverse total shoulder arthroplasty: a biomechanical study. J Shoulder Elbow Surg 21:483-490.

37. Kontaxis A, Johnson GR. 2009. The biomechanics of reverse anatomy shoulder replacement--a modelling study. Clin Biomech (Bristol, Avon) 24:254-260.

38. Ackland DC, Robinson DL, Wilkosz A, et al. 2018. The influence of rotator cuff tears on muscle and joint-contact loading after reverse total shoulder arthroplasty. J Orthop Res (In press).

39. Graichen H, Stammberger T, Bonel H, et al. 2000. Glenohumeral translation during active and passive elevation of the shoulder - a 3D open-MRI study. J Biomech 33:609-613.

40. Wu W, Fong J, Chrocher V, et al. 2018. Modulation of shoulder muscle and joint function using a powered upper-limb exoskeleton. J Biomech (Accepted 31st Jan, 2018).

41. Bacle G, Nove-Josserand L, Garaud P, et al. 2017. Long-Term Outcomes of Reverse Total Shoulder Arthroplasty: A Follow-up of a Previous Study. J Bone Joint Surg Am 99:454-461.

FIGURES

Fig. 1: Testing rig used for muscle moment arm and muscle line of action experiments. Upper limb specimens were mounted to the rig's support frame by potting the scapula in a hollow potting bock filled with dental cement. A marker triad was inserted into the scapula, and a marker cluster inserted into the humerus so that glenohumeral joint motion was visible to an optical motion analysis system. Nylon lines were sutured to the tendon of distal insertion of each muscle-tendon unit and were passed through a perforated backing plate to a free-hanging weight. Each nylon line passed through the backing plate so that the approximate line of action of the muscle-tendon unit was reproduced. Nylon sleeves were inserted into holes in the backing plate to ensure low-friction motion of the nylon line in the hole, and retro reflective markers attached below each free weight to facilitate tendon excursion measurement using the motion analysis system.

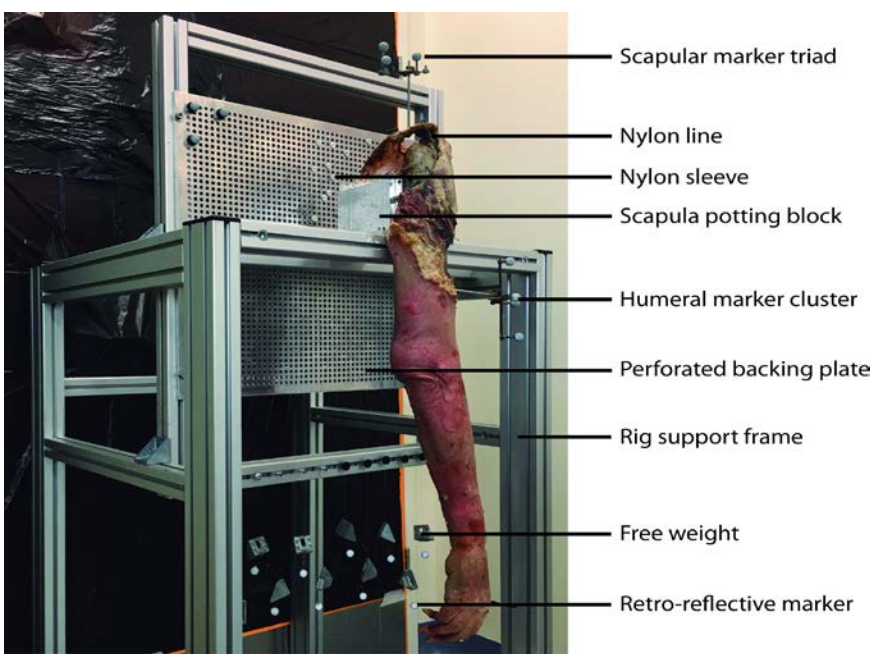

Fig. 2: X-ray fluoroscopy images of a representative shoulder specimen after anatomic total shoulder arthroplasty using a metal-backed modular shoulder system (left image) and the same shoulder after revision reverse total shoulder arthroplasty (right image). Also shown is the approximate joint centre location (green circles) and humeral stem position (yellow circles) that was used to calculate post-operative humeral displacements. A two-dimensional coordinate system centered and aligned with the glenoid plane of the baseplate was used to express muscle lines of action and humeral position (white coordinate system).

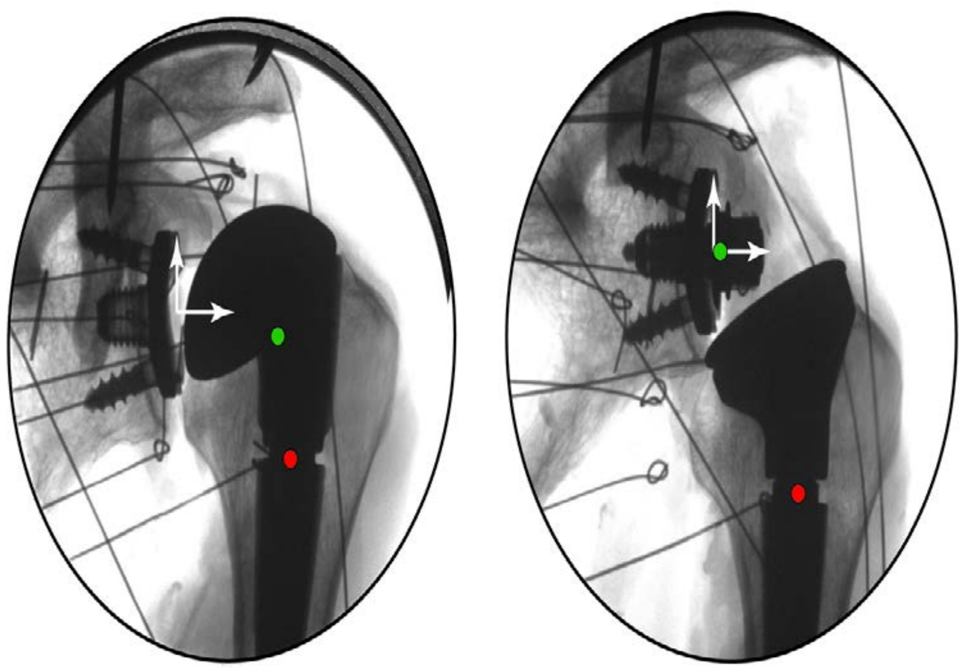

Fig. 3: Illustration of musculoskeletal model of the native shoulder (A) the shoulder after anatomic total shoulder arthroplasty (B) and revision reverse total shoulder arthroplasty (C). Musculoskeletal modelling was used to calculate pre- and post-operative muscle and joint forces during abduction, flexion and axial rotation of the humerus. Red lines indicate muscle paths.

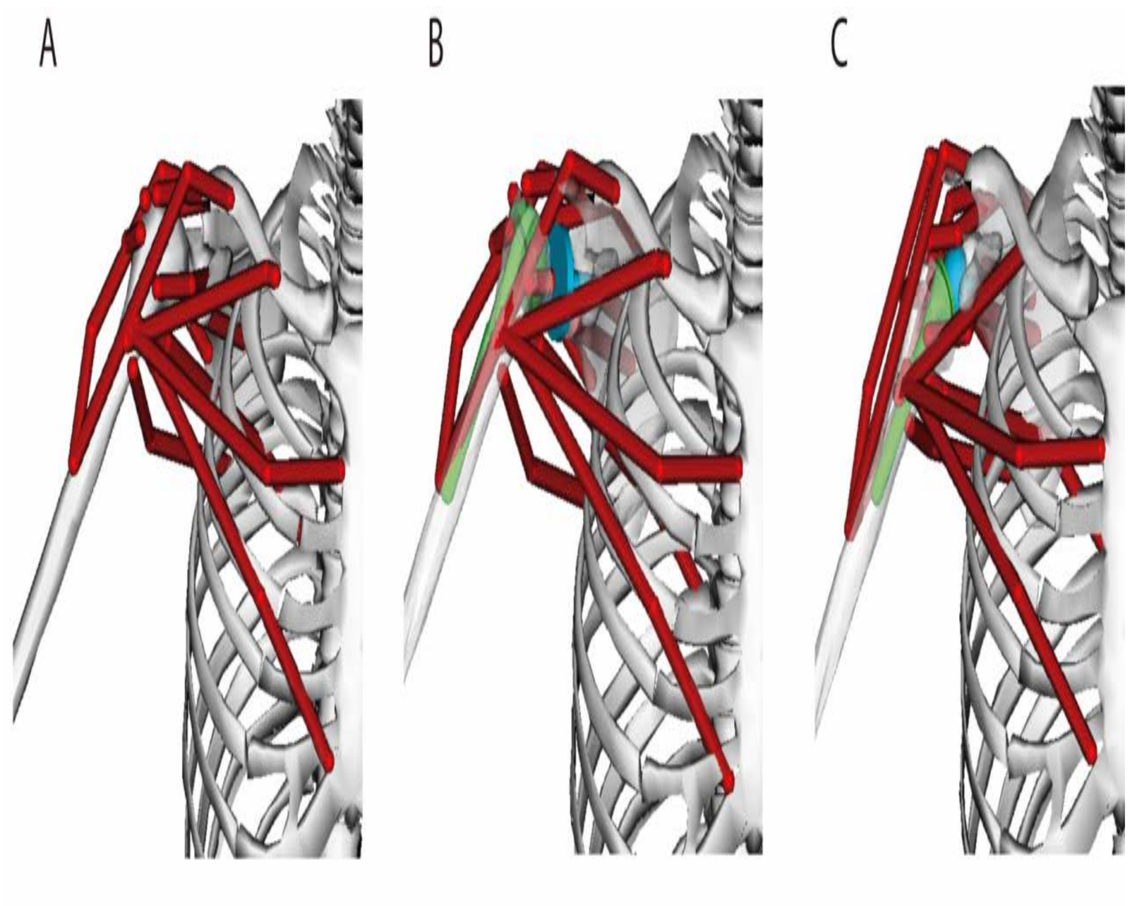

Fig. 4: Muscle lines of action in the scapular plane for the anatomic and reverse shoulder at 0° of humeral abduction. Lines of action are displayed for the anterior deltoid (DeltA), middle deltoid (DeltM), posterior deltoid (DeltP), anterior supraspinatus (SupraA), posterior supraspinatus (SupraP), superior subscapularis (SubsS), middle subscapularis (SubsM), inferior subscapularis (SubsI), superior infraspinatus (InfraS), inferior infraspinatus (InfraI) and teres minor (Tmin). Muscle line of action angles were defined clockwise from the line of action vector to a line parallel to the glenoid base (red arrow). Dashed arrows represent muscle lines of action in the anatomical shoulder, while solid black arrows represent lines of action in the reverse shoulder. Blue circles represent the approximate centroid location of each muscle or sub-region origin.

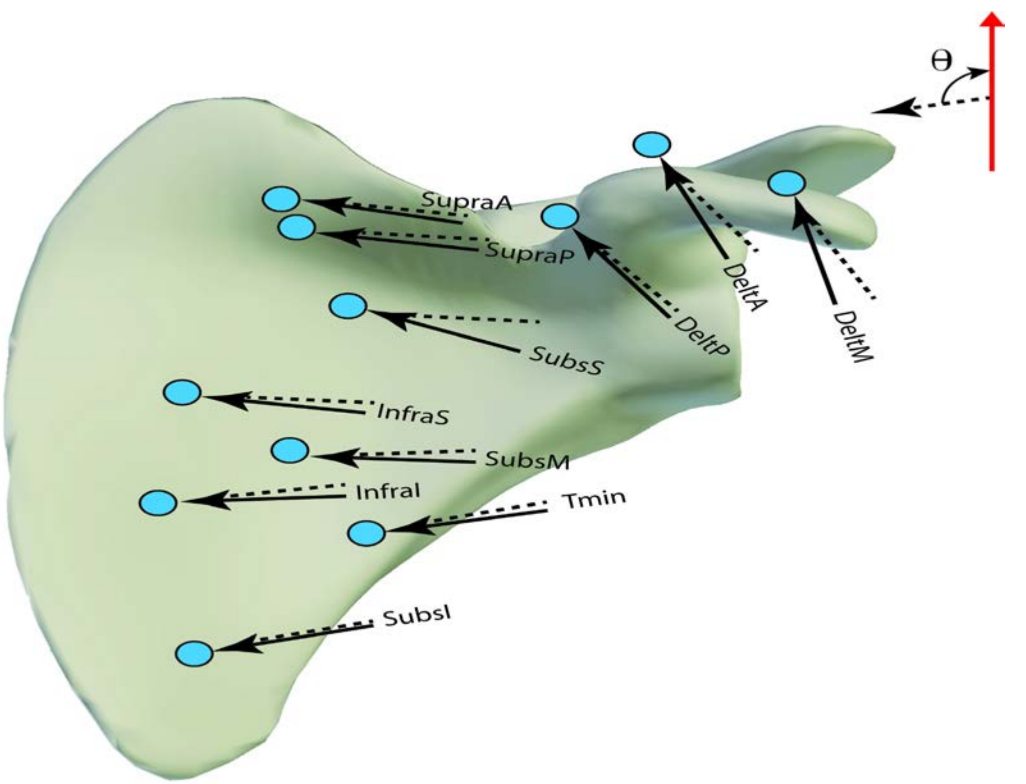

Fig. 5: Selected muscle forces and glenohumeral joint forces (GHJF) calculated during abduction of the humerus in the native shoulder and the shoulder after anatomic total shoulder arthroplasty and revision reverse total shoulder arthroplasty. Positive X, Y and Z joint force directions are anterior, superior and lateral, respectively. Negative X, Y and Z joint force directions are posterior, inferior and medial (compressive), respectively.

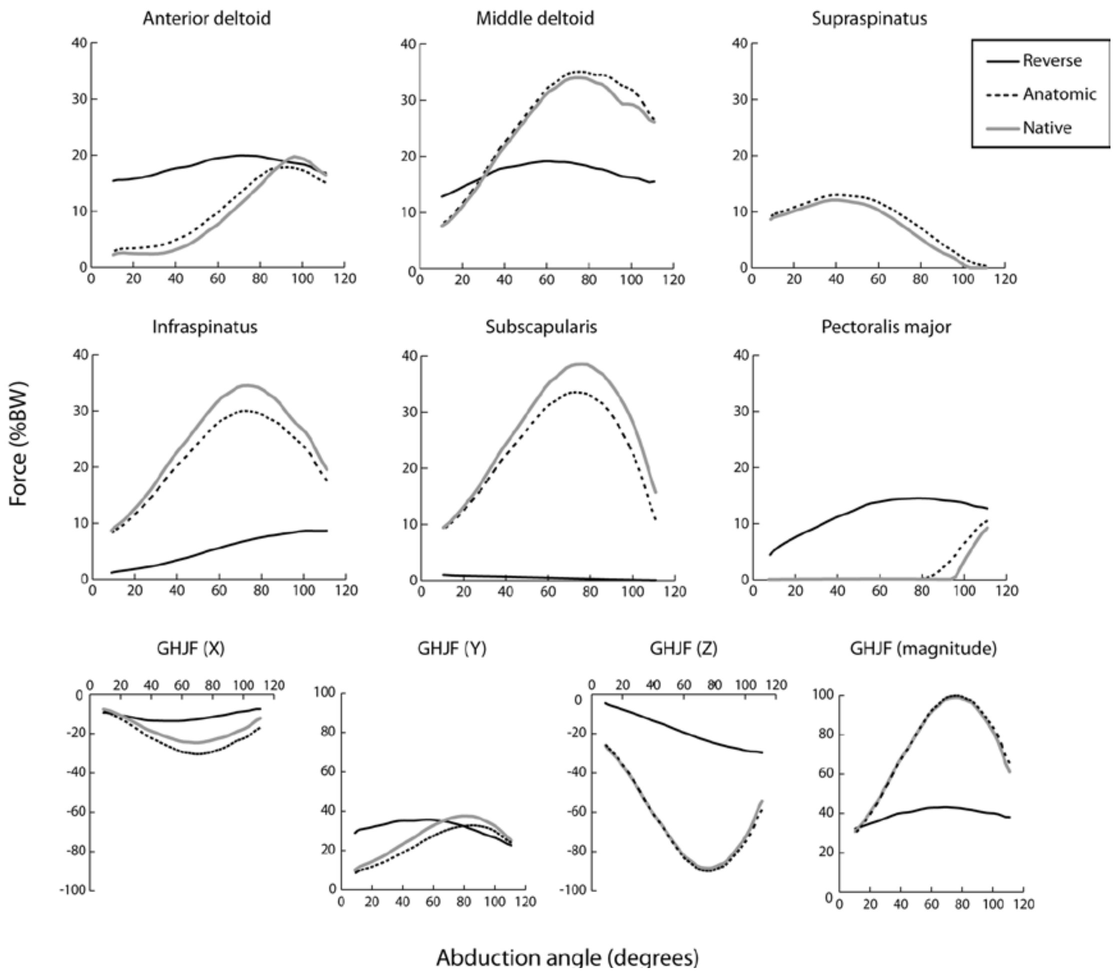

Fig. 6: Selected muscle forces and glenohumeral joint forces (GHJF) calculated during sagittal-plane flexion of the humerus in the native shoulder and the shoulder after anatomic total shoulder arthroplasty and revision reverse total shoulder arthroplasty. See caption of Fig. 3 for definition of joint force directions.

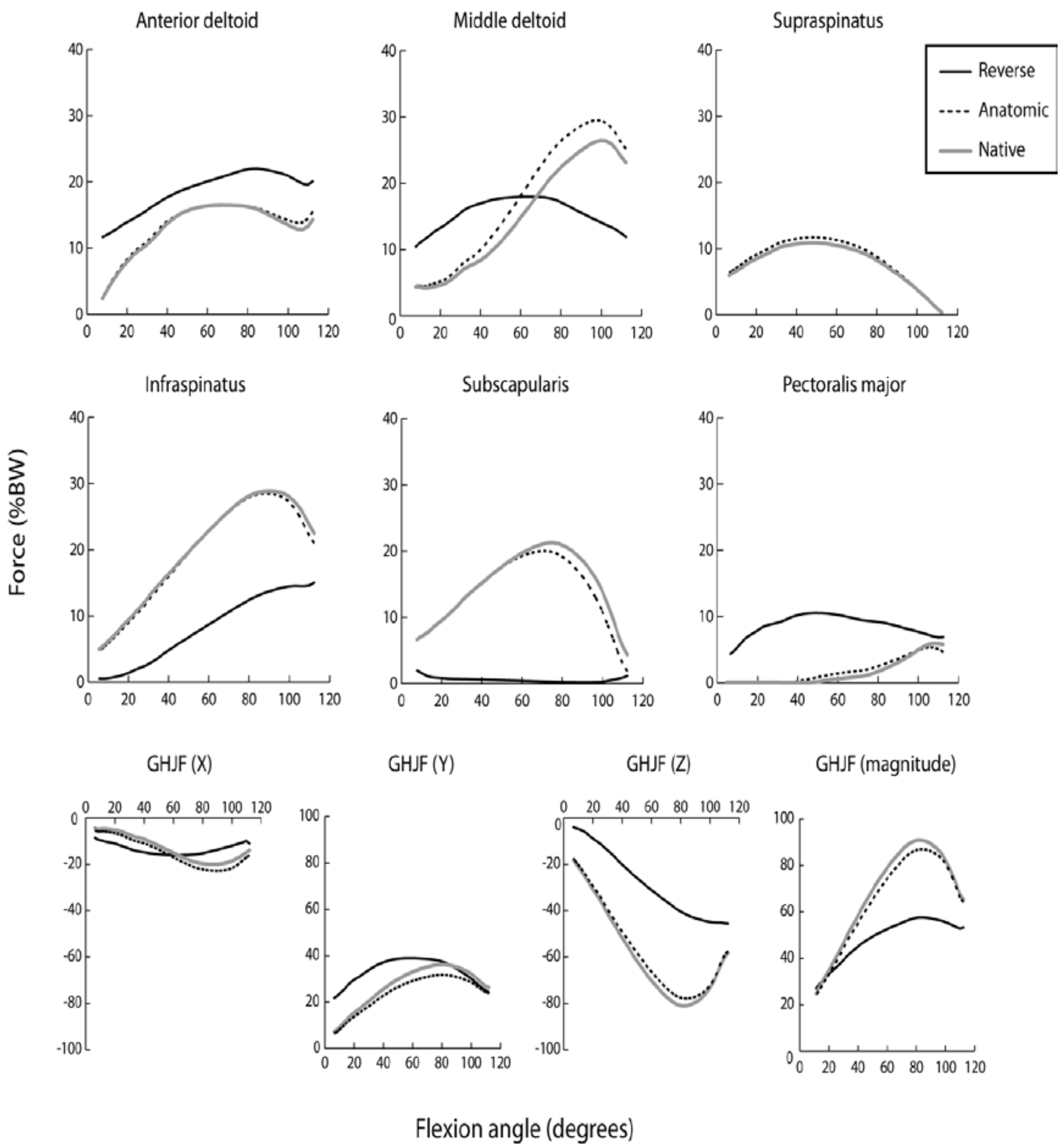

Fig. 7: Selected muscle forces and glenohumeral joint forces (GHJF) calculated during external rotation of the humerus at 45° of abduction. Data are given for the native shoulder and the shoulder after anatomic total shoulder arthroplasty and revision reverse total shoulder arthroplasty. See caption of Fig. 3 for definition of joint force directions.

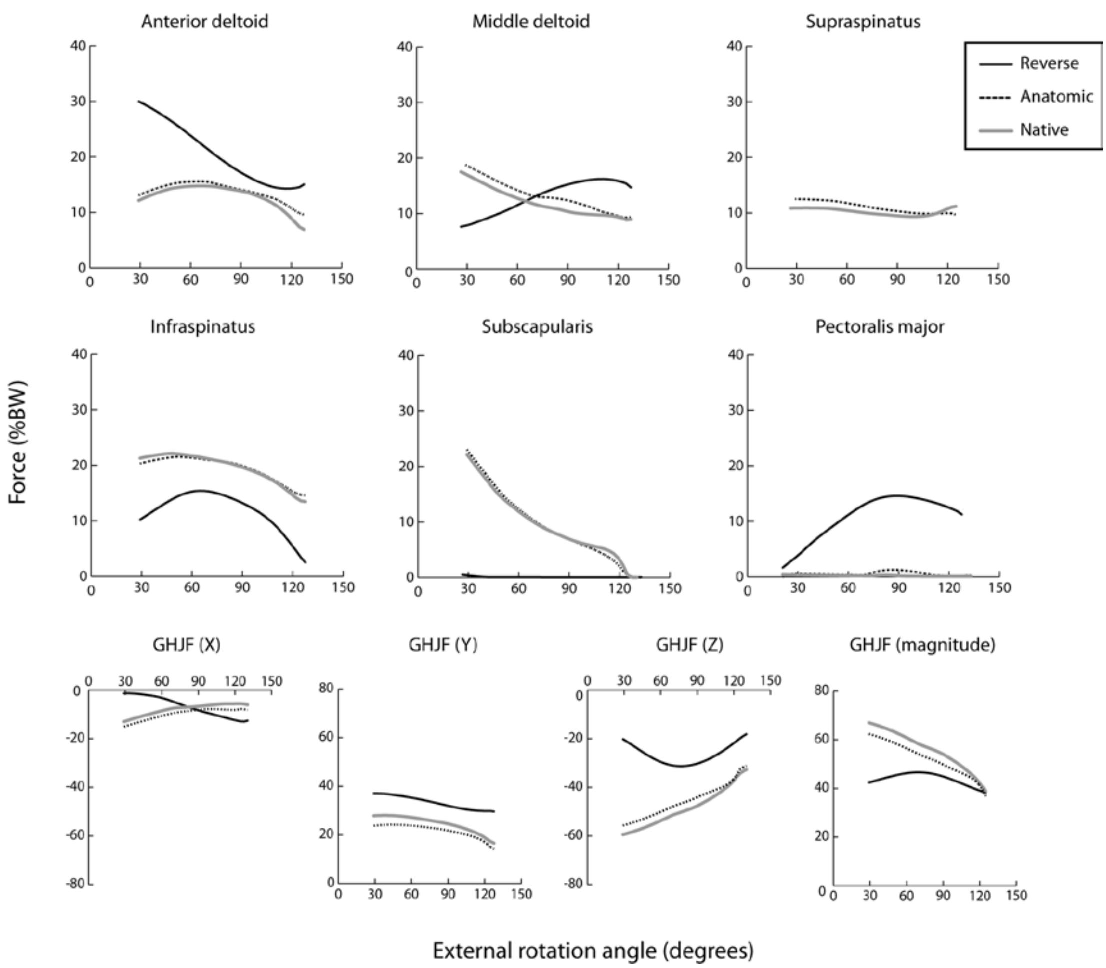

Table 1

	Native						Anatomic						Reverse						Significance	
	Abduction			Flexion			Abduction			Flexion			Abduction			Flexion				
	Max	SD	Angle	Max	SD	Angle	Max	SD	Angle	Max	SD	Angle	Max	SD	Angle	Max	SD	Angle	Abduction	Flexion
Anterior Deltoid	22.1	9.1	96.4	34.1	7.8	47.1	18.3	6.3	94.7	33.3	6.7	14.1	28.2	7.1	89.5	41.2	7.7	43.0	b	c
Middle Deltoid	31.1	5.6	95.4	19.6	15.4	61.1	28.8	7.0	98.4	12.5	14.1	48.9	42.1	8.4	83.0	34.0	18.0	80.5	b, c	b
Posterior Deltoid	-31.6	5.6	6.1	-40.6	12.1	49.1	-23.8	12.1	25.0	-42.8	7.0	31.6	-5.7	5.5	35.6	-31.5	13.0	23.1	b, c	b, c
Anterior Supraspinatus	29.2	2.5	32.3	11.4	6.1	28.2	32.1	6.1	46.6	20.1	12.9	15.9	28.9	6.8	33.1	29.6	18.0	16.3		c
Posterior Supraspinatus	28.0	1.8	31.8	14.4	7.1	17.3	31.2	6.6	47.0	25.9	15.0	12.5	30.5	4.6	28.6	27.6	14.1	10.0		
Superior Subscapularis	-4.9	13.3	91.4	-9.3	6.4	80.2	-2.2	8.5	79.8	-9.0	5.6	38.6	-4.9	5.5	98.9	-8.6	6.4	66.4		
Middle Subscapularis	-10.9	13.3	92.0	-13.5	5.5	68.6	-6.0	12.3	80.8	-15.8	9.1	30.5	-16.2	10.3	73.3	-18.5	14.2	68.4		
Inferior Subscapularis	-17.8	15.9	79.3	-26.3	10.0	53.4	-13.6	13.4	73.1	-32.6	16.5	25.9	-28.8	8.1	74.7	-30.1	18.0	34.7	b	
Superior Infraspinatus	27.9	5.7	72.1	18.0	6.9	68.2	27.2	4.9	75.8	24.7	16.3	66.4	19.5	6.0	61.3	21.0	15.6	85.3	b, c	
Inferior Infraspinatus	25.3	9.6	86.8	15.7	3.3	63.6	24.1	6.3	83.8	23.3	13.0	59.5	15.5	7.9	96.7	15.1	12.2	79.4		
Teres Minor	-18.8	6.3	16.6	6.1	8.2	52.3	-11.3	7.8	20.3	2.4	6.9	40.0	-23.5	9.8	30.6	7.0	9.9	58.0	b	

Table 2

	Native						Anatomic						Reverse						Significance	
	45° Abduction			45° Flexion			45° Abduction			45° Flexion			45° Abduction			45° Flexion			45°	45°
	Max	SD	Angle	Max	SD	Angle	Max	SD	Angle	Max	SD	Angle	Max	SD	Angle	Max	SD	Angle	Abd.	Flex.
Anterior Deltoid	-4.9	3.5	21.4	12.3	6.7	58.3	-7.0	3.1	49.4	12.3	5.7	16.3	-6.3	3.2	79.4	-8.8	1.7	50.7		
Middle Deltoid	8.9	4.9	-39.3	14.9	8.2	36.7	12.3	5.5	-34.4	-8.1	3.3	26.9	12.6	5.6	-31.9	-7.6	5.9	45.0		
Posterior Deltoid	11.9	3.0	-29.3	9.9	1.9	-21.7	12.5	6.7	-23.8	9.4	6.0	-11.9	9.9	3.0	-23.8	6.4	3.5	-11.4		
Anterior Supraspinatus	8.1	2.0	70.0	12.0	4.6	1.7	5.4	4.5	46.9	-7.3	6.6	-27.5	8.8	4.2	14.4	-5.8	6.0	29.3		
Posterior Supraspinatus	10.0	3.8	67.1	-3.9	1.0	-11.7	8.7	3.5	44.4	-3.6	5.4	-7.5	11.4	4.1	-2.5	-4.1	6.4	33.6		
Superior Subscapularis	21.0	2.8	22.1	23.1	2.3	43.3	19.4	2.6	2.5	21.3	5.6	-14.4	16.9	2.8	21.3	19.3	6.8	40.0	c	
Middle Subscapularis	25.6	2.6	27.1	29.1	2.7	53.3	22.4	2.7	-3.8	24.3	6.4	4.4	22.7	4.1	1.3	20.0	6.4	49.3		c
Inferior Subscapularis	28.4	3.4	41.4	26.2	2.5	53.3	24.3	1.9	18.8	23.3	6.4	4.4	25.0	4.5	0.6	20.2	4.4	37.9		
Superior Infraspinatus	20.7	3.0	65.7	14.1	2.7	28.3	19.2	3.6	41.9	16.0	4.9	-3.8	19.2	1.5	20.0	17.7	4.2	22.1		
Inferior Infraspinatus	25.5	2.9	50.0	21.6	3.7	10.0	23.3	4.0	36.3	22.5	6.2	-18.8	22.8	3.3	31.3	23.0	4.6	43.6		
Teres Minor	26.4	2.3	26.4	24.9	4.4	-20.0	25.5	4.0	17.5	22.8	6.7	-15.0	24.4	3.6	18.8	27.0	6.1	23.6		

Table 3

		0°		45°				90°					
		Abduction		Abduction		Flexion		Abduction		Flexion			
		Mean	SD	Mean	SD	Mean	SD	Mean	SD	Mean	SD	Significance	
												Abd.	Flex.
Anterior Deltoid	Anatomical	144.1	11.7	133.8	8.3	139.8	11.0	124.8	5.1	120.1	12.0	a	a
	Reverse	156.0	10.7	142.2	9.0	142.5	9.4	126.1	4.3	127.2	10.4		
Middle Deltoid	Anatomical	151.0	14.5	138.8	12.0	133.4	11.4	114.5	2.9	118.4	13.6	a,b	a,b
	Reverse	165.8	10.2	152.5	9.0	153.1	12.7	131.2	4.6	133.3	17.0		
Posterior Deltoid	Anatomical	140.0	8.5	128.0	12.9	129.4	6.1	110.1	4.1	122.4	4.4	a	a,c
	Reverse	143.6	7.6	129.7	8.5	131.7	6.5	111.0	3.5	113.0	6.3		
Anterior Supraspinatus	Anatomical	98.4	9.4	93.1	11.6	93.5	9.5	92.0	4.7	93.4	11.6	a	a
	Reverse	102.1	5.1	98.4	8.0	99.3	5.3	99.8	2.3	97.1	6.5		
Posterior Supraspinatus	Anatomical	94.7	8.0	92.1	7.8	97.0	6.7	90.7	2.1	99.5	7.2	a	c
	Reverse	98.9	7.2	94.6	7.3	94.3	5.1	91.2	3.6	91.5	7.8		
Superior Subscapularis	Anatomical	94.1	10.6	97.2	8.2	91.5	9.8	92.2	5.9	87.9	12.9	b	a,b
	Reverse	111.8	6.6	108.7	7.8	107.8	5.0	109.8	3.1	108.5	6.0		
Middle Subscapularis	Anatomical	87.1	9.2	85.9	7.9	81.1	5.9	84.1	3.7	79.3	8.0		a
	Reverse	93.0	8.9	93.5	7.0	89.7	6.3	92.8	2.4	88.9	7.9		
Inferior Subscapularis	Anatomical	76.4	11.5	77.0	8.9	70.2	9.1	73.9	1.8	75.7	10.0		
	Reverse	76.7	7.7	75.8	7.6	72.9	6.7	78.2	2.8	74.2	8.5		
Superior Infraspinatus	Anatomical	86.3	5.6	80.2	7.9	89.3	5.7	80.8	3.8	91.2	7.6	a,b	c
	Reverse	98.4	8.4	91.7	10.0	92.7	9.2	85.4	3.2	84.7	8.8		
Inferior Infraspinatus	Anatomical	81.7	6.6	80.6	7.8	85.8	6.2	82.1	2.9	85.6	5.4	c	
	Reverse	87.1	7.2	84.6	6.7	85.3	6.2	77.8	2.5	81.2	4.7		
Teres Minor	Anatomical	76.1	7.1	74.6	6.9	79.8	4.8	73.2	2.7	77.6	6.0	a	c
	Reverse	79.1	7.6	76.8	6.5	79.0	5.0	73.7	2.6	75.8	6.2		

Table 4

	Native						Anatomic						Reverse						Significance		
	Abduction		Flexion		Rotation		Abduction		Flexion		Rotation		Abduction		Flexion		Rotation				
	Mean	SD	Mean	SD	Mean	SD	Mean	SD	Mean	SD	Mean	SD	Mean	SD	Mean	SD	Mean	SD	Abd.	Flex.	Rot.
Anterior Deltoid	9.3	0.0	11.7	0.1	12.5	0.1	10.0	0.5	12.0	0.2	13.5	0.6	16.4	2.5	17.6	1.9	21.0	3.0	a,b,c	a,b,c	a,b,c
Middle Deltoid	23.7	0.2	13.7	0.0	12.2	0.2	24.7	0.9	15.8	1.5	13.2	0.8	16.4	4.0	14.7	5.3	12.7	3.9	a,b,c		
Posterior Deltoid	0.1	0.0	0.4	0.1	0.1	0.0	0.1	0.0	0.4	0.1	0.1	0.0	0.2	0.1	1.2	0.6	0.2	0.1		b,c	b,c
Supraspinatus	7.2	0.0	7.6	0.0	10.2	0.1	8.3	0.8	8.0	0.4	10.9	0.5	0.0	0.0	0.0	0.0	0.0	0.0	a	a	a
Subscapularis	25.5	0.0	13.6	0.1	10.3	0.1	22.3	2.2	12.8	0.6	9.8	0.4	0.5	1.2	0.7	1.1	0.1	0.1	a,b,c	a,b,c	a,b,c
Infraspinatus	23.7	0.1	18.3	0.1	19.4	0.1	21.0	1.8	17.9	0.3	19.3	0.1	5.2	0.9	7.3	1.0	11.1	0.9	a,b,c	a,b,c	b,c
Teres minor	0.0	0.0	0.1	0.0	0.2	0.0	0.0	0.0	0.3	0.1	0.3	0.1	0.0	0.0	0.4	0.3	0.7	0.4	a	a	c
Trapezius	10.2	0.1	7.2	0.0	8.1	0.0	10.4	0.2	7.4	0.1	8.3	0.1	10.1	0.3	6.9	0.2	7.9	0.2	a	a,b,c	a,b
Pectoralis major	1.0	0.0	1.4	0.0	0.2	0.0	1.7	0.5	1.6	0.2	0.6	0.3	11.4	1.3	8.1	1.6	10.8	1.4	a,b,c	a,b,c	a,b,c
Serratus anterior 1	12.0	0.1	9.0	0.0	9.4	0.0	12.3	0.2	9.2	0.2	9.6	0.2	12.2	0.4	8.8	0.3	9.5	0.3	a	a,b	a
Rhomboids minor	3.4	0.0	1.4	0.0	3.1	0.0	3.5	0.0	1.4	0.0	3.2	0.0	3.0	0.1	1.0	0.1	2.7	0.1	a,b,c	a,b,c	a,b,c
Joint force (Anterior)	-21.4	0.1	-13.9	0.1	-10.2	0.2	-17.4	2.8	-12.0	1.4	-8.0	1.6	-10.9	3.7	-12.8	5.5	-6.4	3.7			
Joint force (Superior)	22.8	0.1	21.9	0.0	21.4	0.1	26.3	2.5	24.7	2.0	24.3	2.0	31.1	4.6	31.9	4.5	33.4	5.2	a,c	a,b,c	a,b,c
Joint force (Compressive)	-64.2	0.3	-51.6	0.2	-46.0	0.4	-63.4	0.5	-53.7	1.7	-48.5	1.9	-18.0	1.6	-25.5	2.9	-25.7	2.5	a,b,c	a,b,c	a,b,c
Joint force (Magnitude)	71.5	0.3	57.8	0.3	51.8	0.4	71.0	0.4	60.4	2.0	54.9	2.3	38.6	5.6	44.6	6.9	43.2	6.1	a,b,c	a,b,c	a,b,c

Table 5

	Native						Anatomic						Reverse						Significance		
	Abduction		Flexion		Rotation		Abduction		Flexion		Rotation		Abduction		Flexion		Rotation				
	Max	SD	Max	SD	Max	SD	Max	SD	Max	SD	Max	SD	Max	SD	Max	SD	Max	SD	Abd.	Flex.	Rot.
Anterior Deltoid	19.7	0.0	16.5	0.1	14.8	0.0	18.5	0.7	16.4	0.1	15.6	0.6	20.0	2.1	22.1	1.5	30.9	4.8		b,c	a,b,c
Middle Deltoid	34.0	0.3	26.5	0.0	18.3	0.2	33.2	1.2	29.6	2.3	19.3	0.8	19.1	4.9	18.2	6.9	16.3	4.5	b,c	a,b,c	
Posterior Deltoid	0.1	0.0	0.8	0.2	0.2	0.0	0.2	0.0	0.9	0.2	0.2	0.1	0.2	0.1	2.2	1.2	0.4	0.2		b,c	b,c
Supraspinatus	12.1	0.0	10.9	0.0	11.2	0.3	13.0	0.7	11.7	0.7	12.5	1.2	0.0	0.0	0.0	0.0	0.0	0.0	a	a	
Subscapularis	38.5	0.1	21.3	0.1	25.5	0.1	33.6	3.3	20.1	0.8	24.5	0.6	1.1	2.5	3.0	1.2	0.7	1.7	a,b,c	a,b,c	a,b,c
Infraspinatus	34.5	0.2	28.9	0.2	22.1	0.1	30.0	3.0	28.5	0.2	21.6	0.4	5.8	1.4	15.0	2.1	15.4	1.2	a,b,c	a,b,c	a,b,c
Teres minor	0.0	0.0	1.1	0.0	1.1	0.3	0.0	0.0	2.2	0.7	1.5	0.5	0.0	0.0	1.2	1.1	3.5	3.2		a	
Trapezius	12.3	0.1	7.7	0.0	10.0	0.1	12.6	0.3	7.9	0.1	10.1	0.2	12.4	0.4	7.4	0.2	9.7	0.3		a,b,c	a,b
Pectoralis major	9.2	0.1	5.9	0.0	0.4	0.0	10.5	0.9	5.4	0.4	1.3	0.6	14.5	1.1	10.5	1.6	14.6	2.0	a,b,c	a,b,c	a,b,c
Serratus anterior 1	15.4	0.2	10.8	0.1	11.5	0.1	16.0	0.5	11.1	0.2	11.7	0.2	15.9	0.6	10.6	0.3	11.0	0.3	a	a,b	a,b,c
Rhomboids minor	3.7	0.0	3.1	0.0	3.8	0.0	3.8	0.1	3.2	0.0	3.9	0.1	3.3	0.1	2.9	0.2	4.0	0.1	a,b,c	a,b,c	a,c
Joint force (Anterior)	-30.4	0.1	-22.3	0.2	-16.4	0.1	-24.7	4.0	-20.0	2.0	-13.6	2.0	-13.6	4.7	-17.1	7.8	-12.3	4.4	a,b,c	a	a
Joint force (Superior)	32.9	0.2	31.8	0.0	24.2	0.1	37.7	3.5	36.3	3.3	28.1	2.8	33.8	5.2	39.0	5.2	37.3	5.6		a,c	a,b,c
Joint force (Compressive)	-89.3	0.4	-77.9	0.4	-56.7	0.3	-88.4	0.8	-81.0	2.5	-60.0	2.5	-29.7	3.9	-46.2	6.2	-31.3	3.5	a,b,c	a,b,c	a,b,c
Joint reaction force (Magnitude)	100.0	0.5	87.0	0.4	63.4	0.4	99.1	0.6	91.0	3.1	67.5	3.2	43.2	3.9	57.7	8.4	46.7	6.9	a,b,c	a,b,c	a,b,c